1. AGI	2. REPORT DATE	3. REPORT TYPE AND DATES COVERED
	23 January 1994	Interim 22-23 January 1994

4. TITLE AND SUBTITLE

Gradient Index Lens Multimode Fiber Probe for Laser Induced Breakdown in the Eye

5. FUNDING NUMBERS

PR - 2312
TA - A1
WU - 01
PR - 7757
TA - 02
WU - 14

6. AUTHOR(S)

Cynthia A. Toth Kim Slawinski
Daniel X. Hammer

7. PERFORMING ORGANIZATION NAME(S) AND ADDRESS(ES)

AL/OEO
Occupational and Environmental Health Directorate
Brooks AFB TX 78235

8. PERFORMING ORGANIZATION REPORT NUMBER

AL/OE-PC-1993-0048

9. SPONSORING/MONITORING AGENCY NAME(S) AND ADDRESS(ES)

10. SPONSORING/MONITORING AGENCY REPORT NUMBER

11. SUPPLEMENTARY NOTES

12a. DISTRIBUTION/AVAILABILITY STATEMENT

Approved for public release; distribution is unlimited.

12b. DISTRIBUTION CODE

13. ABSTRACT *(Maximum 200 words)*

A model laser surgical probe was designed and built to employ laser induced breakdown (LIB) in cutting fibrovascular membranes within the vitreous cavity of the eye. Current surgical techniqes for removing such membranes from eyes with severe proliferative diabetic retinopathy or similar proliferative retinopathies involve cutting the membranes with microscissors or other micro-cutting devices. The mechanical movement of scissor blades may damage adjacent tissues directly or by shearing and traction. A laser cutting system that uses optical breakdown would reduce such mechanical damage but may introduce collateral laser damage.

The probe is a simple design of a gradient index (GRIN) lens attached to the tip of a multimode fiber. It is designed to fit through a sclerotomy incision and enter the vitreous cavity for work anterior to the retina. The laser light is focused close to the tip of the probe without causing GRIN lens damage. Thus a widely divergent beam behind the focus will diminish potential laser damage posterior to the target tissue.

A Nd:YAG 1064 nm 10ns pulsed laser was used with the probe inserted into a cell of tap water. Threshold data for laser induced breakdown was taken and fit to a probit curve. The data was compared with past LIB threshold data.

14. SUBJECT TERMS	15. NUMBER OF PAGES
Gradient Index(GRIN) lens, Laser Induced Breakdown(LIB), Proliferative Diabetic Retinopathy, laser surgical probe	14
	16. PRICE CODE

17. SECURITY CLASSIFICATION OF REPORT	18. SECURITY CLASSIFICATION OF THIS PAGE	19. SECURITY CLASSIFICATION OF ABSTRACT	20. LIMITATION OF ABSTRACT
Unclassified	Unclassified	Unclassified	UL

PROCEEDINGS REPRINT

SPIE–The International Society for Optical Engineering

Reprinted from

Proceedings of

Ophthalmic Technologies IV

22–23 January 1994
Los Angeles, California

P

Volume 2126

Gradient Index (GRIN) lens multimode fiber probe for laser induced breakdown in the eye

Cynthia A. Toth[1], Daniel X. Hammer[2], Kim Slawinski[3], and Gary D. Noojin[4]

[1] Duke University Eye Center, Durham, NC 27710
[2] AL/OEO, Brooks AFB, Texas 78235-5215
[3] Wilford Hall Medical Center, San Antonio, Texas 78236-5300
[4] The Analytic Science Corporation, San Antonio, Texas 78235

ABSTRACT

A model laser surgical probe was designed and built to employ laser induced breakdown (LIB) in cutting fibrovascular membranes within the vitreous cavity of the eye. Current surgical techniques for removing such membranes from eyes with severe proliferative diabetic retinopathy or similar proliferative retinopathies involve cutting the membranes with microscissors or other micro-cutting devices. The mechanical movement of scissor blades may damage adjacent tissues directly or by shearing and traction. A laser cutting system that uses optical breakdown would reduce such mechanical damage but may introduce collateral laser damage.

The probe is a simple design of a gradient index (GRIN) lens attached to the tip of a multimode fiber. It is designed to fit through a sclerotomy incision and enter the vitreous cavity for work anterior to the retina. The laser light is focused close to the tip of the probe without causing GRIN lens damage. Thus a widely divergent beam behind the focus will diminish potential laser damage posterior to the target tissue.

A Nd:YAG 1064 nm 10 ns pulsed laser was used with the probe inserted into a cell of tap water. Threshold data for laser induced breakdown was taken and fit to a probit curve. The data was compared with past LIB threshold data. The radiant exposure versus distance from the probe was plotted via spot size measurements. This measurement gave a rough indication of the distance the probe must remain from the retina to be well below retinal maximum permissible exposure (MPE) levels. In vitro threshold measurements of bovine vitreous[1] were taken and compared to the water threshold. Finally, collagen membranes were lased with the probe to demonstrate its functional application.

2. INTRODUCTION

The surgical treatment of many vitreoretinal diseases involves removal of membranes or vitreous strands overlying the surface of the retina. Current techniques use mechanical micro-cutting devices to sever the attachments of these membranes. Despite significant advancements in techniques and instruments, the mechanical movement of scissor blades or aspirating-cutting systems may damage adjacent tissues directly or through shearing and traction forces. This study is concerned with developing a laser delivery system with a microfocusing probe placed within the vitreous cavity for laser cutting of fibrovascular membranes or vitreous strands during vitreoretinal surgery. The gradient index lens (GRIN, SELFOC, Nippon Sheet Glass, Inc.) was evaluated for microfocusing to cut membranes by either LIB or direct irradiance of tissue. We chose to evaluate the potential for laser induced breakdown (LIB) using this probe system. GRIN lenses have been utilized in medicine as components of endoscopic systems[2], in laser delivery for retinal photocoagulation[3] and in laser angioplasty[4], however, these applications did not involve LIB.

LIB of tissue has been used effectively in ophthalmic surgery for puncturing the opaque posterior capsule (capsulotomy) after cataract surgery, puncturing the iris to relieve intraocular pressure (iridotomy) in glaucoma, and severing opaque strands or sheets within the anterior vitreous humor[5]. In these

0-8194-1419-0/94/$6.00

procedures, the laser source is external to the eye with pupil size and the refractive power of the cornea and lens playing an important role in the location of the focus of the laser light. Because the laser light is focused in the anterior portion of the eye, lower irradiance in the posterior segment decreases the damage potential to the retina. External delivery systems for LIB are not currently used in the operating room for vitreoretinal surgery.

Several laser techniques have previously been evaluated for intraocular membrane cutting and removal. Such techniques have utilized erbium-YAG[6] and holmium-YAG[7] with fiberoptic focusing for membrane ablation by direct irradiance. Others have utilized pulsed laser with focusing fiberoptic for LIB[8], and in some cases for transection of intraocular membranes[9].

One problem with these laser treatments is the potential for damage to the underlying retina and retinal pigment epithelium both of which may be less than 500 μm posterior to the membrane. Damage can occur from transmitted laser energy which is absorbed in the underlying structures, thermal heating adjacent to treatment site, gas expansion and movement, or a shifting of plasma formation site. A microfocusing probe placed within the vitreous may decrease retinal damage by providing better localization of plasma (in the case of LIB) or better energy delivery (in the case of direct irradiance) with steeper convergence and thus wider divergence beyond the focal area. Laser wavelength could also be selected to diminish transmission of energy through the vitreous and/or diminish retinal and RPE absorption. Pulsed laser may be utilized for LIB with the potential for less thermal damage adjacent to the treatment site and for plasma shielding from optical breakdown. The use of LIB, however, adds the hazard of gas formation and cavitation effects.

3. LASER INDUCED BREAKDOWN

Laser induced breakdown is a process by which atoms are ionized and a plasma of quasi-free electrons and ions is created. In optical breakdown, ionization is induced by optical absorption and lasts approximately the duration of the pulse creating it. With LIB in liquid, there is plasma expansion, where optical absorption produces superheating, further ionization, vaporization of non-ionized liquid and thermal expansion. Second, there is plasma collapse, where cooling produces plasma emission in the form of a spark, liquid vaporization at the plasma edge, and electron-ion recombination. Third, resulting from the plasma expansion, hypersonic shock waves propagate through the media. Finally, resulting from the plasma collapse, a caviation bubble forms and collapses during cooling. The cavitation bubble collapse causes small but visible bubbles to stream from the breakdown site.

LIB initiation occurs by one of two ionization mechanisms, avalanche or multiphoton. Avalanche ionization occurs when a seed electron absorbs photons, accelerates, and frees bound electrons by collisional ionization. These electrons in turn accelerate and free more electrons, and the process cascades into a volume of plasma. Avalanche ionization is likely to occur in the ns time regime where the pulse is relatively long, compared to the collisional ionization time, and present in the lens focal region for an extended period of time for the cascade to propagate. This mechanism is highly impurity dependent. Multiphoton ionization occurs when each bound electron is freed by absorption of multiple photons. Each electron acts independently and no particle interactions are needed. Multiphoton ionization is likely to occur in the fs time regime and a transition between the two processes occurs the ps time regime. With multiphoton ionization, electrons are stripped and ions are created simultaneously with very little impurity concentration dependence. Pulse irradiances in the fs regime are sufficiently high enough to ionize water molecules by multiphoton ionization with little regard for the readily available electron-donating impurities[10].

4. DEVICE DESIGNS

4.1 Probe 1 Design

The preliminary design tested the feasibility of achieving LIB with the laser light coupled directly into a 1.8 mm diameter 0.23 pitch GRIN lens (probe 1). This preliminary design was used to remove the complications involved with coupling light into the fiber and from the fiber through the GRIN lens.

4.2 Probe 2 Design

The second iteration of design yielded a GRIN multimode fiber probe (probe 2). This simple design consisted of a 1.8 mm diameter 0.23 pitch GRIN lens attached to a tapered fiber (made by Fiberguide, Inc.). The fiber tapers from 200 μm core/220 μm cladding to 100 μm core/110 μm cladding. An air-tight outer metal flange surrounds the lens and fiber to preserve the distance between the fiber and lens and to provide support. There is an air gap between the fiber and lens to maintain the proper working distance of the device.

4.3 GRIN lens selection

GRIN lenses bend light in a manner similar to conventional lenses, however, they use a difference in index of refraction within the lens rather than a difference in axial thickness of the lens (Snell's Law) to bend the light (Figure 1). Therefore, the focusing of the GRIN lens is not dependent on the diameter of the lens and the lens can be made very small. The index of refraction of the GRIN lens is defined as follows.

$$N(r) = N_0\left(1 - \frac{A}{2}r^2\right) \qquad (1)$$

where r = radial distance from optical axis
A = gradient constant (squared)
N_0 = refractive index at optical axis

For most applications, the refractive index decreases radially from the optical axis. Both A and N_0 are dependent on wavelength.

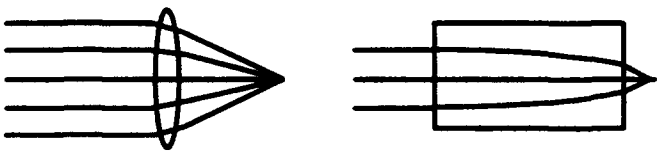

Conventional Lens Cylindrical GRIN Lens

Figure 1: Conventional lens vs GRIN Lens (2-D view from side)

Light travels through the GRIN lens sinusoidally according to the pitch length of the lens (Figure 2). The pitch is the optical length of the lens. A pitch length equal to one is defined as the length it takes the light to complete one cycle while traveling through the lens. For example, a half pitch lens will focus and recollimate light that is collimated upon entering the lens and a quarter pitch lens will focus collimated light at the front face of the lens. The actual length of the lens, Z is related to the pitch, P as follows.

$$Z = \frac{2\pi P}{\sqrt{A}} \qquad (2)$$

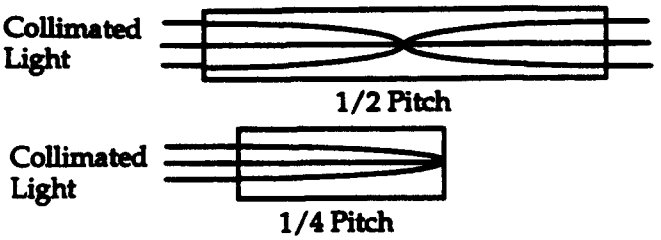

Figure 2: Cross section of GRIN lens showing different pitches

The working distance of the lens or lens to image distance, L_2 is defined as the distance from the back surface of the lens to the focal point. The object to lens distance, L_1 is defined as the distance from the source (in this case the fiber) to the lens. These distances are related as follows.

$$L_2 = \frac{1}{N_0\sqrt{A}}\left(\frac{N_0L_1\sqrt{A}\cos\sqrt{A}Z + \sin\sqrt{A}Z}{N_0L_1\sqrt{A}\sin\sqrt{A}Z - \cos\sqrt{A}Z}\right) \quad (3)$$

Equation (3) omits consideration of the aberrations which cause the focal volume to spread and move. In addition, it assumes the refractive index at the input and output of the lens is 1.0. In our case the index of refraction at the output face of the GRIN lens is 1.3. Using a matrix raytracing program, we have predicted that the focal point will move further away from the lens than that predicted by equation (3).

The numerical aperture of a lens is the sine of the half angle of the acceptance cone. The acceptance cone is the area that will best transmit light through the lens. For a GRIN lens, the numerical aperture is maximum at the optical axis and decreases with distance from the axis. The numerical aperture at the optical axis is calculated as follows.

$$NA_{max} = \sin\theta_{max} = \sqrt{AN_0^2r_0^2} \quad (4)$$

where r_0 = radius of the lens (mm)

Standard GRIN lenses are available with three different numerical apertures, 0.37, 0.46, and 0.60 corresponding to standard (S), wide (W), and high (H) field of view. The numerical apertures will vary slightly with wavelength.

The magnification of the lens is the ratio of image size to object size. For a GRIN lens, the magnification is calculated as follows.

$$M = \sqrt{\frac{N_0^2L_2^2A+1}{N_0^2L_1^2A+1}} \quad (5)$$

The magnification will also change if the indices of refraction at the front and back surface are not 1.0.

A more complete description of GRIN lenses can be found in the NSG Reference Manual[11] and "Selected Papers on Gradient-Index Optics"[12].

For probe 2 design, we will take the fiber core size to be the object size. Hence, the spot size at the focus of the probe is determined by the fiber size and the distances between the fiber and lens. A magnification of 0.5 was chosen to achieve minimum spot size within the limitations of optimal object to

lens and lens to image distances for our application. At lower magnification, the numerical aperture of the lens will prohibit efficient coupling. At higher magnification, large energies are required to breakdown the media due to the large spot size. For a magnification of 0.5, the following distances are calculated for various pitches from equation (3) and (5).

Table I: Object and image distances for various pitches

Pitch	0.23	0.25	0.29
L_1 (mm)	4.09	3.82	3.45
L_2 (mm)	1.23	0.98	0.54

The pitch was chosen by the following considerations. First, L_2 must be kept large enough to avoid damage to the GRIN lens. Second, L_1 must be kept small enough so all the divergent light will fill the entire area of the lens. In order to fill the entire area of the lens, the following must hold true.

$$L_1 \tan(\sin^{-1}(\text{N. A.})) < .35d \qquad (6)$$

where N. A. = output numerical aperature of the fiber
d = diameter of the GRIN lens

With a fiber output numerical aperture of 0.22, the 0.29 pitch will provide the best coupling at L_1 for the manufacturer's recommended 60%-70% of the lens face. However, damage to the lens is a more pressing consideration in our design. Therefore, a 0.23 pitch lens was chosen for the probe.

4.4 Fiber Selection

The irradiance needed for breakdown of the vitreous is calculated from the spot size, the pulse duration, and the energy. In order to achieve breakdown, we have to balance minimum spot size and the damage threshold of the fiber. The damage threshold of the fiber is calculated as follows[13].

$$E = 440 d^{.95} t^{.5} \qquad (7)$$

where d = fiber diameter (mm)
t = pulse duration (s)

Past data taken on LIB have given irradiance levels required to achieve breakdown in various media. Due to the probabilistic nature of LIB, these levels are usually reported as either a 50% or 100% probability for breakdown. Docchio, et al.[14] have reported the 100% probability irradiance threshold of breakdown for various pulse durations and spot sizes. With a magnification of 0.5 as specified above, we chose the fiber that had the highest damage threshold and lowest breakdown threshold. Table II tabulates the breakdown of tap water and damage thresholds for spot sizes similar to those we are interested in.

Table II: Breakdown Thresholds Reported[14] and Damage Thresholds Calculated[13]

Pulse Duration (ps)	Spot Size (d, μm)	Breakdown threshold (mJ)	Fiber size (μm)	Damage threshold (mJ)	Coupling efficiency needed
7000	50	0.55	100	4.13	13.3%
			tapered	7.98	6.9%
7000	94	2.52	200	7.98	31.6%
7000	350	20.20	600	22.66	89.1%
220	45	0.90	100	0.73	-
			tapered	1.42	63.4%
220	120	0.68	200	1.42	47.9%
30	45	0.33	100	0.27	-
			tapered	0.52	63.5%
30	120	0.17	200	0.52	32.7%

The table indicates with a reasonable amount of coupling, we can build a fiber/lens probe for a laser with 7 ns pulse duration for a 200 μm, 100 μm, or 200/100 μm tapered fiber. However, the coupling efficiency needed for the 600 μm fiber is not realistically achievable. For the 220 ps pulse duration, high coupling efficiency is required for the tapered and 200 μm fibers. The damage threshold of the 100 μm fiber is greater than the breakdown threshold, so 100 % breakdown is physically unattainable. The values for the efficiency needed for 30 ps are similar to those of 220 ps.

Upon exiting the fiber, the laser light has a cone of divergence from its core diameter. The cone of divergence relates to the numerical aperture in the same way that the cone of acceptance relates to the numerical aperture of a GRIN lens. In order to optically match the fiber to the lens the numerical aperture of the lens has to be equal to or exceed the numerical aperture of the fiber. The output numerical aperture of the fiber is 0.22. The numerical aperture of a type W GRIN lens is 0.46. Therefore, the lens will gather all the output light of the fiber as long as the fiber and lens are within the distances listed above. The primary consideration in the design is the light loss due to the large distance between the fiber and the lens.

Figure 3 shows a diagram of the fiber probe. Figure 4 shows a photograph of the fiber probe.

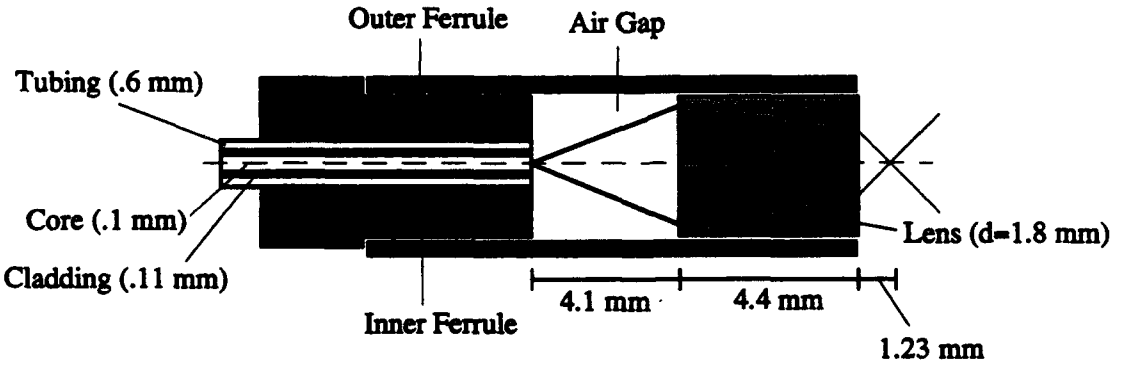

Figure 3: Diagram of fiber probe (Drawing not to scale)

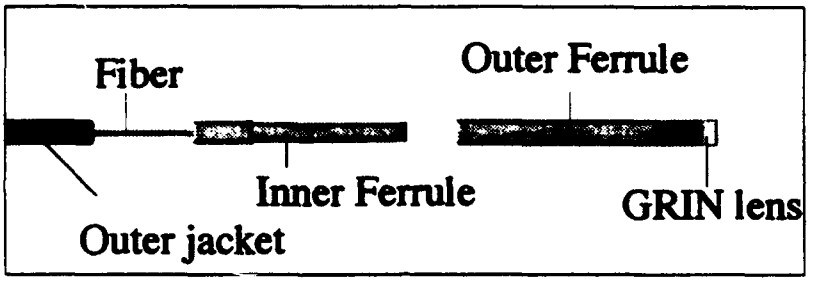

Figure 4: Picture of Fiber/Grin Probe

The following is a summary of the SELFOC micro lens and fiber characteristics chosen.

GRIN Lens characteristics:
$N_O = 1.5940$
$\sqrt{A} = 0.329\ mm^{-1}$
$P = 0.23$
$Z = 4.39$ mm
$M = 0.5$
$L_2 = 1.23$ mm
$L_1 = 4.09$ mm
N. A. = 0.46

Fiber characteristics:
Multimode graded index tapered fiber
input core diameter = 200 μm
input cladding diameter = 220 μm
output core diameter = 100 μm
output cladding diameter = 100 μm
Output N. A. = 0.22
Input N. A. = 0.11
Acrylate jacket

5. EXPERIMENTAL SETUP

The optical setup for probe 2 is shown in Figure 5. Two different lasers are used for the different pulse durations required. The ultrashort pulse laser system, described by Cain[15], produces 80 ps pulses at 1064 nm and variable (single shot to 10 Hz) pulse repetition frequency. This system was used to record the spot sizes with the knife edge measurement technique described in section 6.3. In addition, this system will be used to test the probe with picosecond pulses. The Spectra-Physics DCR-11 Nd:YAG produces 10 ns pulses at 1064 nm and variable (single shot to 10 Hz) pulse repetition frequency. The energy output of either laser is controlled with a 1/2 wave plate and polarization cube. The energy detectors used were either J50, J25, or J4 Molectron detectors output to a Molectron JD2000 Joulemeter Ratiometer. The light is aligned through two apertures with two mirrors to control the x position, y position, angle, and tilt. The ratio of beamsplitter BS1 is B/A1. Once this is calculated, the light is focused onto the SMA connectorized fiber held in the fiber coupler. The light is focused onto the coupler

with different lenses depending on the fiber size. The fiber and lens focus the light approximately 1.23 mm in front of the device. The coupling efficiency of the device is calculated by multiplying the ratio of detector A2 to detector B by the ratio of BS1. The energy that enters the probe is found by multiplying the inverse beamsplitter ratio, A1/B, with the readings from detector B. The energy that exits the probe immersed in the cuvette of media is found by multiplying the coupling efficiency by the energy that enters the probe. This energy must remain above the breakdown threshold for laser induced breakdown.

The setup for probe 1 differs only slightly from that of probe 2. Light from the laser was recollimated with two lenses to the diameter of the GRIN lens and delivered to probe 1 with the output end immersed in a cuvette of tap water. Tap water has been shown to have comparable optical properties to vitreous[16]. Bovine vitreous is also used for comparison. The energy that enters probe 1 is found in a similar manner as probe 2. The laser is then pulsed at increasing energies until breakdown is achieved. The breakdown event was recorded on videotape with a Hitachi CCTV Camera.

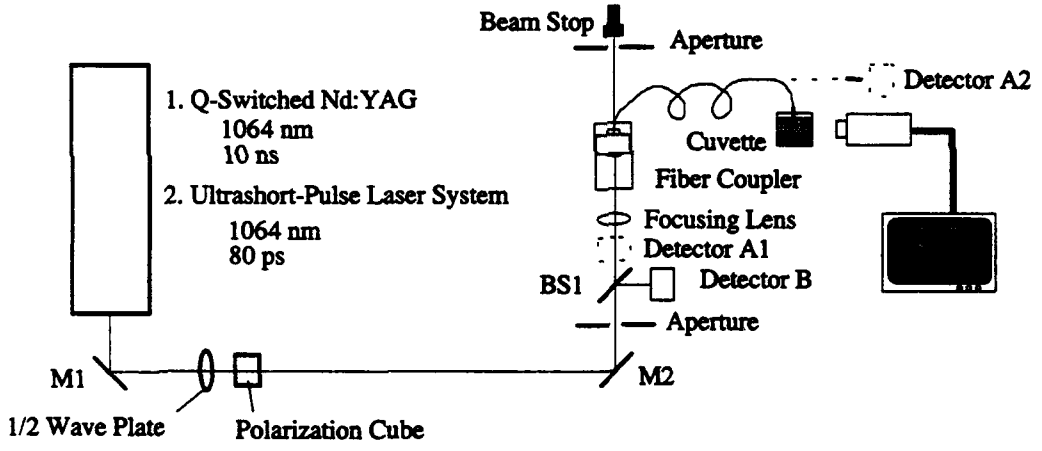

Figure 5: Optical Setup

6. RESULTS AND DISCUSSION

6.1 Variations in Design

The design for probe 2 presented thus far should give LIB when a certain threshold energy is reached providing there is efficient coupling of laser light into the fiber. We have not been able to reach the thresholds for breakdown even though we have surpassed the theoretically predicted energies needed. Therefore, the following results and discussion of LIB thresholds were taken with probe 1. The spot size measurements were performed on the both probes. We believe LIB is attainable with probe 2, providing a nonlinear mechanism or other effect of passing high energy through the fiber is preventing breakdown.

6.2 Probit Analysis

Due to the probabilistic nature of LIB, a method of calculating the thresholds for breakdown based upon a normal distribution of data points is needed. Probit analysis[17] is one means of calculating the probability of breakdown versus energy dose delivered to a cuvette of media. Probit curves and fiducial limits were computed on Statistical Analysis System (SAS). Probit curves give the probability that an energy dose will cause breakdown. The probability is usually reported as an ED_{xx} value which gives the xx% probability that a certain event will occur. In addition, probit analysis gives fiducial limits of the probability which express the confidence limits of a probability.

6.2.1 Probit curves for LIB with Probe 1 in tap water and vitreous

Figure 6 shows the probit curves that were generated from the LIB threshold values measured for tap water and bovine vitreous with probe 1. The 95% fiducial limits were omitted from the figure for clarity. Due to the pulse duration of the laser, the area of the plasma formation can be quite large and increases with increasing energy[18,19]. If the plasma area exceeds approximately 2 mm and extends backward to touch the lens, the lens will be damaged. Therefore, in order to get enough data for a probit analysis, care was taken not to exceed the damage threshold of the lens. A precise damage threshold measurement was not taken because of the number of devices at our disposal but it was found to be approximately 4 mJ. The lens was viewed under a microscope following measurements to insure no damage occurred to the lens during the experiment. The ED_{99} values for tap water and bovine vitreous were 1.08 mJ and 1.01 mJ, respectively. These measured thresholds are comparable to LIB threshold measurements done in the past[20,21].

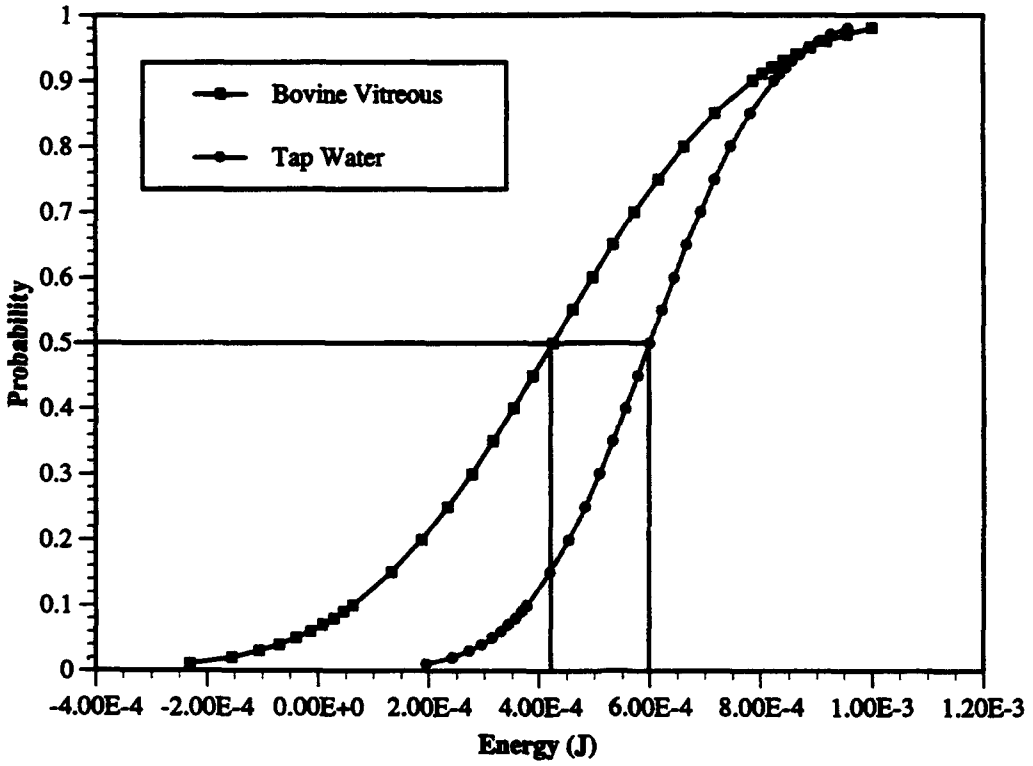

Figure 6: Probit Curves for tap water and bovine vitreous

6.3 Spot size calculations

In order to get a true measure of the irradiance of the plasma, a spot size analysis was performed with both probes. The spot size was measured by scanning a knife edge through the transverse axis of the beam (y direction) at different points along the longitudinal axis of the beam (x direction). By detecting and recording the light which passed the knife edge, a curve representing the width of the beam was generated. By taking clip levels of 16% and 84%[22,23], we obtained the $1/e^2$ radius of the beam at points along the longitudinal axis of the beam. With successive iterations, the spot size was found. In addition, we could measure the radius of the beam at any distance from the lens.

An Aerotech Unidex 11 Motion Controller was used with a resolution of 0.1 μm in the x direction and 0.01 μm in the y direction. The spot size measurements were taken in air and will be different in water or vitreous. Future testing of the probes will involve a spot size determination in vitreous and water Figure 7 shows the spot sizes calculated for both probes at their focal points. Figure 8 shows the beam diameter calculated for each probe at a far-field distance from the back surface of the GRIN lens. Figure 9 shows the radiant exposure calculated at different points along the optical axis of the GRIN lens at the ED_{50} and ED_{99} energy levels and the calculated retinal maximum permissible exposure without the optical gain of the eye[24,25].

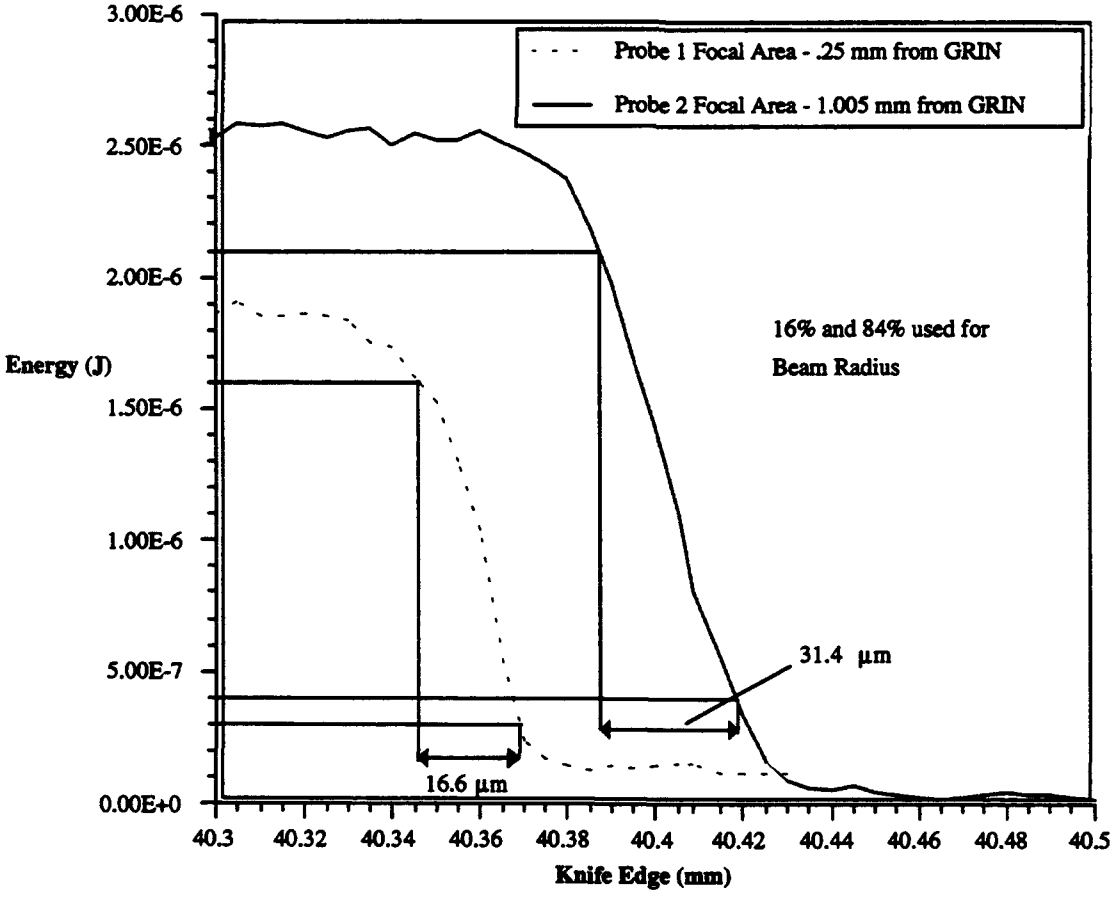

Figure 7: Spot Size for Probe 1 and Probe 2 at their focal points

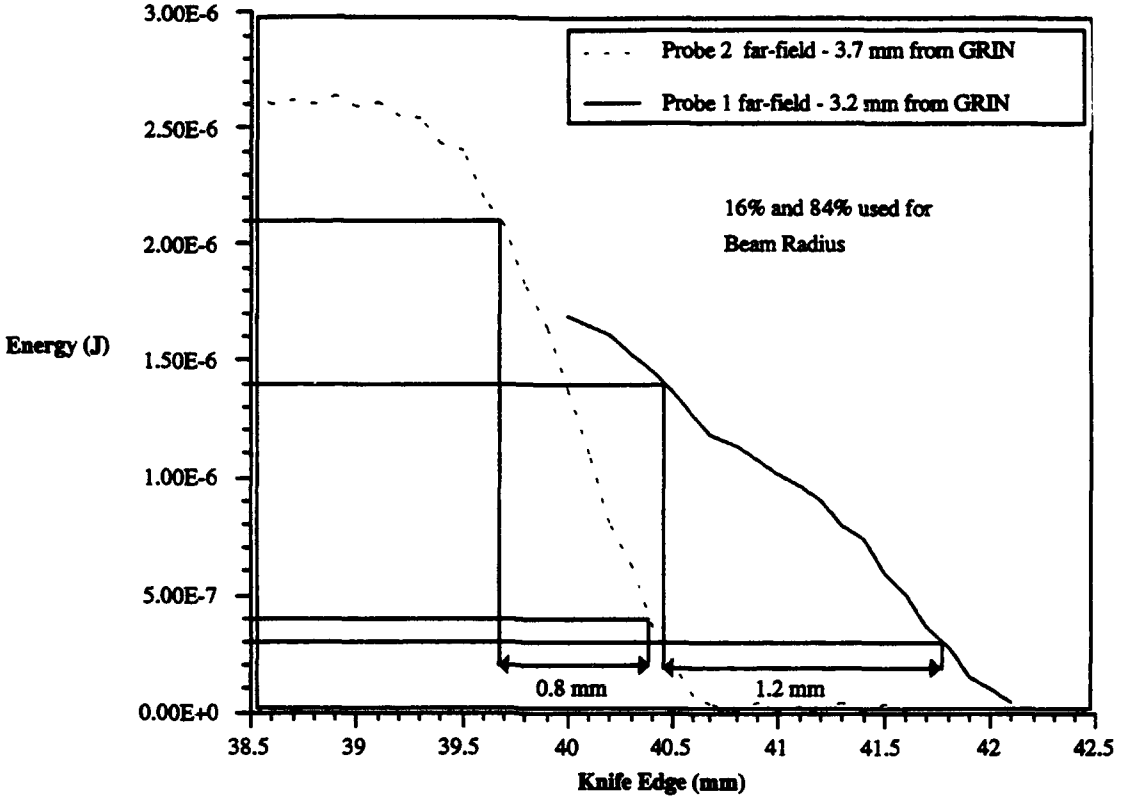

Figure 8: Spot size for Probe 1 and Probe 2 far from GRIN lens

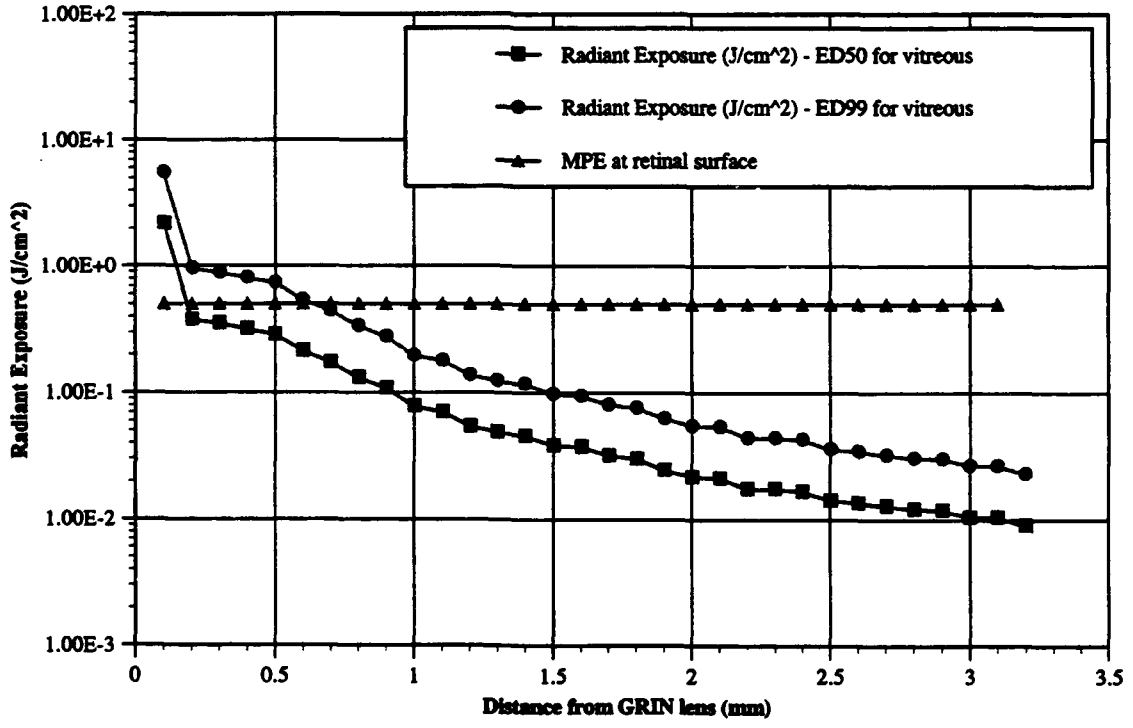

Figure 9: Radiant Exposure calculations from spot size measurements

6.4 Functional capabilities

We demonstrated that probe 1 could produce ED_{99} for LIB in water and vitreous at laser levels below that of lens damage. Plasma formation was videorecorded on VHS videotape. Images of the plasma were observed to occur at approximately 0.6 mm from the output surface of the GRIN lens (Figure 10). This was 1/2 the distance predicted by L_2 (Table I) yet was twice the distance predicted by the spot size measurements (Figure 7). The videoimage may, however, erroneously predict the location of LIB, due to camera pixel saturation and because the image documents longer time frame events occurring after LIB.

The functional capability of probe 1 was further demonstrated by testing the probe on a clear collagen sheet (Bio-Cor 72 hour Collagen Corneal Shield, Bausch and Lomb) held by a flexible metal suspender immersed in water adjacent to the probe tip. With energy of 1.2 to 2.2 mJ, numerous holes were created in the sheet. Rupture sites were viewed with a light microscope at 400X, and demonstrated a star shaped rupture site in the sheet (Figure 11).

Probe 2 is awaiting further testing.

Figure 10: Plasma Formation at the distal tip of the GRIN lens

6.5 Discussion

One of the concerns with the use of laser cutting tools near the retina is the hazard from laser energy transmitted past the treatment site to the underlying retina and RPE. Absorption of this energy by the retina and RPE may cause damage. With probe 1 we measured the radiant exposure at selected distances posterior to the focal area (Figure 9) and demonstrated a significant drop in radiant exposure over the first 200 μm beyond the focal area. Further, the radiant exposure was seen to drop below the MPE levels for 1064 nm laser energy for points greater than 500 μm from the focal area.

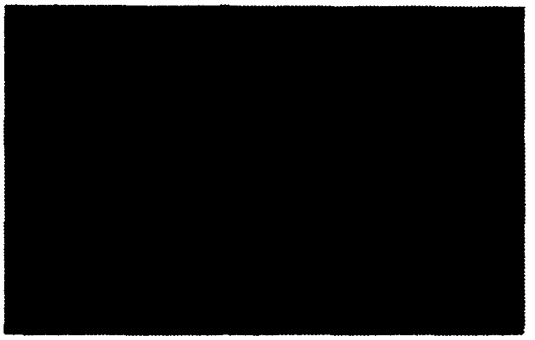

Figure 11: Star shaped damage to collagen shield (view parallel to the laser propagation direction)

6.6 Future refinements

There are many advantages to using this device in laser surgery. It is very easy to control the laser light with this instrument. Light is focused rapidly, and diverged rapidly. Thus the device can be used close to the retina. It can be used with existing ophthalmic laser systems. It is small enough to be inserted into the eye. In addition, it is inexpensive and can be disposable. Moreover, the ability to place the LIB site anywhere in the eye may lead to future application. One disadvantage of the device is it is easily damaged if the LIB threshold is exceeded by a large amount. This can be controlled by setting the energy to a level slightly larger than the LIB threshold but below the damage threshold.

There are many future refinements to be considered for this system. Some might involve consideration of alternative wavelengths and pulsewidths with appropriately matched fibers and GRIN lenses. Others might involve selection of different GRIN lens parameters to provide better focusing. Spherical aberrations might be reduced and thus a tighter focus attained by using a plano-convex GRIN lens that has a curved surface on one end. A lens of diameter 1.0 mm can be used to make the probe even smaller for entry into the eye via typical surgical sclerotomies of approximately 1 mm. The smaller the device, the less collateral damage the instrument will induce. Finally, with fiber technology progressing at rapid speed, more efficient fibers or fibers with higher damage thresholds may be used for the high energies required.

Other LIB effects, such as shock wave generation and bubble formation, need to be studied to assess any danger in causing LIB so close to the retina. This paper only covered one, the irradiance thresholds calculated from spot size and energy measurements. Future experiments are planned for performing this type of surgery with the device inserted into a rabbit's or monkey's eye to determine the feasibility of using this device for human laser surgery. Preliminary measurements show a lot of promise.

7. ACKNOWLEDGMENTS

This work was supported by AFOSR and PL/LIDA. We would especially like to thank Sylvia Mancha at Phillips Laboratory. We would also like to thank all those who helped with the theory and testing of the instrument, including Randy Thompson, Rex Eiserer, John Mileski, and Pat Roach.

8. REFERENCES

1. Animals involved in this study were procured, maintained, and used in accordance with the Animal Welfare Act and the "Guide for the Care and Use of Laboratory Animals" prepared by the Institute of Laboratory Animal Resources, National Research Council.
2. D. C. Leiner, R. Prescott, "Correction of chromatic aberrations in GRIN endoscopes," Applied Optics, Vol. 22, No. 3, p. 383, 1983

3. M. M. Pankratov, O. Pomerantzeff, K. P. Pflibsen, G. R. Bearse, "A Step-Zoom Probe for Laser Endophotocoagulation: I. Design," *Ophthalmic Surgery*, Vol. 18, p. 61, 1987
4. D. Decker-Dunn, D. A. Christensen, G. M. Vincent, "Multifiber Gradient-Index Lens Laser Angioplasty Probe," *Lasers in Surgery and Medicine*, Vol. 10, p. 85, 1990
5. S. J. Gitomer, R. D. Jones, "Laser-Produced Plasmas in Medicine," *IEEE Transactions on Plasma Science*, Vol. 19, p. 1209, 1991
6. T. I. Margolis, D. A. Farnath, M. Destro, C. A. Puliafito, "Erbium-YAG Laser Surgery on Experimental Vitreous Membranes," *Archives of Ophthalmology*, Vol. 107, p. 424, 1989
7. S. Borirakchanyavat, C. A. Puliafito, G. H. Kliman, T. I. Margolis, E. L. Galler, "Holmium-YAG Laser Surgery on Experimental Vitreous Membranes," *Archives of Ophthalmology*, Vol. 109, p.1605, 1991
8. P. Rol, P. Niederer, F. Fankhauser, M. Arigoni, E. De Haller, "Q-Switched pulses and optical breakdown generation through optical fibers," *Lasers and Light in Ophthalmology*, Vol. 3, No. 3, p. 213, 1990
9. S. M. Meyers, R. F. Bonner, M. M. Rodriques, E. J. Ballantine, "Phototransection of vitreal membranes with the carbon dioxide laser in rabbits," *Ophthalmology*, Vol. 90, p. 563, 1983
10. P. Kennedy, S. A. Boppart, "Optical Breakdown: A Conceptual Overview," Talk given at Brooks AFB on 8 March 1993
11. *SELFOC Product Guide*, NSG America Inc.
12. D. T. Moore, Ed., Selected Papers on Gradient-Index Optics, The Society of Photo-Optical Instrumentation Engineers, Vol. MS67, Bellingham, Washington, 1993
13. *Laser Delivery Nomograph (Pulsed Lasers)*, Fiberguide Industries Application Note
14. F. Docchio, C. A. Sacchi, and J. Marshall, "Experimental investigation of optical breakdown thresholds in ocular media under single pulse irradiation with different pulse durations," *Lasers in Ophthalmology*, Vol. 1, No. 2, p. 83, 1986
15. C. P. Cain, "Ultrashort-Pulse Laser System: Theory of Operation and Operating Procedures," *Armstrong Laboratory Technical Report*, AL-TR-1991-0146
16. E. F. Maher, "Transmission and Absorption Coefficients for Ocular Media of the Rhesus Monkey," *School of Aerospace Medicine Technical Report*, SAM-TR-78-32, 1978
17. D. J. Finney, Probit Analysis, Cambridge University Press, Third Edition 1971
18. B. Zysset, J. G. Fujimoto, T. F. Deutsch, "Time-Resolved Measurements of Picosecond Optical Breakdown," *Applied Physics B*, Vol. 48, p. 139, 1989
19. F. Docchio, P. Regondi, M. R. C. Capon, J. Mellerio, "Study of temporal and spatial dynamics of plasmas induced in liquids by nanosecond Nd:YAG laser pulses," *Applied Optics*, Vol. 27, No. 17, p. 3661, 1988
20. F. Docchio, C. A. Sacchi, "Nd:YAG Laser Irradiation of an Eye Model: Experimental Analysis," *Lasers in Surgery and Medicine*, Vol. 6, p. 520, 1987
21. J. G. Fujimoto, W. Z. Lin, E. P. Ippen, C. A. Puliafito, R. F. Steinert, "Time Resolved Studies of Nd:YAG Laser-Induced Breakdown," *Investigative Ophthalmology and Visual Science*, Vol. 26, p. 1771, 1985
22. A. E. Siegman, M. W. Sasnett, T. F. Johnston, Jr., "Choice of Clip Levels for Beam Width Measurements Using Knife-Edge Techniques," *IEEE Journal of Quantum Electronics*, Vol. 27, No. 4, 1991
23. T. F. Johnston, Jr, "M^2 concept charcterizes beam quality," *Laser Focus World*, Vol. 26, No. 5, 1990
24. D. Sliney and M. Wolbarsht, Safety with Lasers and Other Optical Sources, Plenum Press, New York, First Edition, 1980
25. *American National Standards for Safe Use of Lasers*, ANSIZ136.1-1993